BIOMATERIALS

The structure of DNA by direct imaging

10.1126/sciadv.1500734

Monica Marini,[1] Andrea Falqui,[2] Manola Moretti,[1] Tania Limongi,[1] Marco Allione,[1] Alessandro Genovese,[2] Sergei Lopatin,[3] Luca Tirinato,[1] Gobind Das,[1] Bruno Torre,[1] Andrea Giugni,[1] Francesco Gentile,[4]* Patrizio Candeloro,[4] Enzo Di Fabrizio[1,4]†

The structure of DNA was determined in 1953 by x-ray fiber diffraction. Several attempts have been made to obtain a direct image of DNA with alternative techniques. The direct image is intended to allow a quantitative evaluation of all relevant characteristic lengths present in a molecule. A direct image of DNA, which is different from diffraction in the reciprocal space, is difficult to obtain for two main reasons: the intrinsic very low contrast of the elements that form the molecule and the difficulty of preparing the sample while preserving its pristine shape and size. We show that through a preparation procedure compatible with the DNA physiological conditions, a direct image of a single suspended DNA molecule can be obtained. In the image, all relevant lengths of A-form DNA are measurable. A high-resolution transmission electron microscope that operates at 80 keV with an ultimate resolution of 1.5 Å was used for this experiment. Direct imaging of a single molecule can be used as a method to address biological problems that require knowledge at the single-molecule level, given that the average information obtained by x-ray diffraction of crystals or fibers is not sufficient for detailed structure determination, or when crystals cannot be obtained from biological molecules or are not sufficient in understanding multiple protein configurations.

INTRODUCTION

This work originates from four questions: (i) Is it possible to obtain a direct image (in the direct space) of a single DNA molecule? (ii) Can a direct image contain quantitative information on the characteristic lengths of the DNA? (iii) Is the preparation followed to obtain the DNA image compatible with its physiological conditions? (iv) Can this method be useful for studying local DNA modification, its protein interactions, and its protein structures, which cannot be obtained by diffraction methods?

The instrument of choice to solve these tasks is the high-resolution transmission electron microscope (HRTEM) with spherical aberration (C_S) correction of the objective lens. In material science, imaging with a resolution of ~1 Å can be realized on a wide category of "hard" samples. In biological molecule imaging, the full exploitation of the C_S-corrected HRTEM meets a series of hurdles mainly related to the low contrast due to the low Z atomic number of the constituting elements and the low density of the sample. Both of these characteristics make biological samples very easy to be radiation-damaged under the usual electron dose range needed to achieve an acceptable signal-to-noise ratio in the final HRTEM images. For these reasons, the proper choice of the HRTEM imaging conditions is crucial for the success of the approach (*1*). In previous works, we proposed a preparation method based on a superhydrophobic microstructured substrate (*2*, *3*) to have a scattering-free image with the highest signal-to-noise ratio (*4*). As a result, we were able to directly image the A-form of the double-strand (ds) λ-DNA (A-DNA) (*5*) and measure its period, which is equal to 27 Å. Here, we achieve a subperiod resolution that reveals the inner structure of A-DNA by improving several aspects of the sample preparation: higher purification, a larger number of suspended fibers, increased reproducibility, and, finally, single dsDNA fiber suspension.

RESULTS

A-DNA direct image and metrology

The TEM image is reported in Fig. 1, with the metrology throughout its four panels. In particular, we show the direct image of a single dsDNA, highlighting the characteristic lengths and other relevant features such as the diameter, major and minor groove visualization, their relative distance, inter–base pair distance, base pair length, and angle measured between the base pair and the helix axis (*5*–*9*). The A-DNA micrograph was taken in a C_S-corrected HRTEM operating at 80 keV electron beam energy, with a magnification of about 1 million and a resolution of 1.5 Å, calculated according to the equations reported in (*10*).

Figure 1A shows about two periods of a single dsDNA in detail. Notice that the reference scale bar is set at 20 Å. Figure 1A represents the outermost dsDNA molecule bound on a 100 Å bundle diameter. The image acquisition time is 1 s, and the electron flux measured at the detector (number of electrons per second and per square angstrom) is equal to 50 e/s Å^2. In the picture, the backbone and the base pairs are clearly distinguishable, despite a slight overlap with another helix located in a second back plane.

In Fig. 1B, the dashed lines fit the winding of the backbone of the double helix. From this picture, the major and minor grooves and period are clearly visible and measurable; the pitch of the helix is equal to 26.5 Å, and the distance between the major and minor grooves is G = 18 Å. The ratio between the helix diameter that corresponds to the minor and major grooves is about 2.0.

In Fig. 1C, the principal characteristic lengths of the dsDNA in the A-form are highlighted. From the figure, we measure the backbone length (A_1 and A_2, where $A_1 = A_2$) that corresponds to the equatorial

[1]SMILEs Lab, Physical Science and Engineering (PSE) and Biological and Environmental Science and Engineering (BESE) Divisions, King Abdullah University of Science and Technology, Thuwal 23955-6900, Kingdom of Saudi Arabia. [2]NABLA Lab, BESE Division, King Abdullah University of Science and Technology, Thuwal 23955-6900, Kingdom of Saudi Arabia. [3]Imaging and Characterization Core Lab, King Abdullah University of Science and Technology, Thuwal 23955-6900, Kingdom of Saudi Arabia. [4]Bio Nanotechnology and Engineering for Medicine (BIONEM), Department of Experimental and Clinical Medicine, University of Magna Graecia, Viale Europa, Germaneto, 88100 Catanzaro, Italy.
*Present address: Department of Electrical Engineering and Information Technology, University of Naples, 80125 Naples, Italy.
†Corresponding author. Email: enzo.difabrizio@kaust.edu.sa

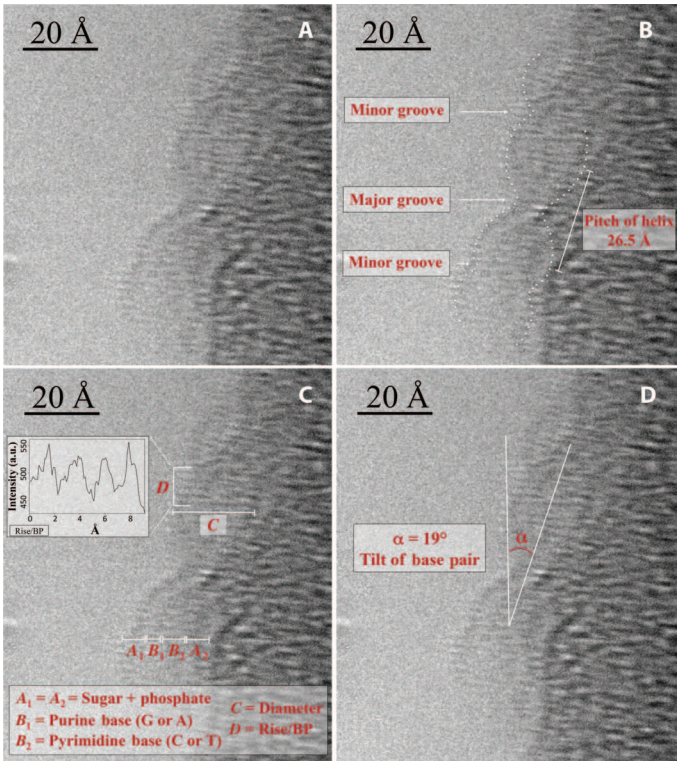

Fig. 1. A-DNA direct image and metrology. (**A**) HRTEM phase-contrast image of a single A-DNA helix bound to a 100 Å DNA bundle obtained by stacking two images acquired with 50 e/s Å^2 at 80 keV. (**B**) Dotted line sharpens the DNA location. Major and minor grooves and the helix pitch of 26.5 Å are highlighted. (**C**) The principal lengths (the backbones, the base pairs (BPs), the diameter, and the rise per base pair) are indicated and reported in Table 1. The length difference between the purine and pyrimidine bases is also shown: a.u., arbitrary unit. (**D**) The tilt of the base pairs with respect to the helix axis is reported and measures 19°.

position, where the double helix reaches its maximum length (DNA diameter *C*, which is equal to 21.2 Å). Here, the backbone length is ~5 Å according to the sum of the lengths of the phosphate and the deoxyribose sugar. The base pair can be distinguished by the length of each complementary base. $B_1 \neq B_2$ (B_1 represents the purine base, whereas B_2 represents the pyrimidine base), where B_1 = 3.6 Å and B_2 = 5.2 Å (*11*, *12*). This is particularly significant because this difference will be important for future studies in fundamental structural biology. The rise of *D* in the base pairs along the helix axis ranges from 2.40 to 2.45 Å. This is clearly measurable in the position of the helix, where the base pairs are almost in the incidence plane of the incoming TEM plane wave (note that the rotation of each base pair is 33°) (*13*).

The last important quantitative information we can obtain from the TEM image is the orientation of the helix. From Fig. 1D, in particular, we measure the angle α between the helix axis and the normal to the base pair, being α = 19°. This is the distinctive spatial configuration of dsDNA when humidity drops below 75% (*9*, *14*, *15*). All these values are summarized in Table 1; in the third column, we report the x-ray accepted data and modeling values for comparison with our direct imaging. We notice that five new molecular structures are measured in the present study. Finally, we notice from Fig. 1 that the variable intensity contrast in the inner of the helix, which we attribute to the base pairs, is

Table 1. A-DNA structural lengths. Relevant measured lengths of A-DNA, as obtained by imaging data reported in Fig. 1 (see inset), are shown. The data reported for HRTEM imaging are coherent and comparable with the x-ray accepted values (*13*–*15*, *30*) and the simulations shown in Fig. 2.

A-DNA structural characteristics	HRTEM measurements* (Å)	X-ray and simulation data (Å)
Diameter	21.2	23.0†
Rise/base pair along axis	2.5	2.6†
Pitch/tum of helix	26.5	28.2†
Phosphate + sugar (backbone A_1)	5.1	5.3‡
Base (B_1)	3.6	4.0‡
Base (B_2)	5.2	5.4‡
Phosphate + sugar (backbone A_2)	5.0	5.3‡
Base length (B_1 + B_2 + base interdistance)	11.3	11.5‡
Tilt of base pair relative to the axis	19°	19°†

*The statistical error for the measured lengths is estimated to be 1.5 Å from the inset of Fig. 1. †X-ray accepted values of relevant lengths as reported in (*13*–*15*, *30*). ‡Data obtained from the simulation of the twisted bases of Fig. 2 and as reported in (*13*).

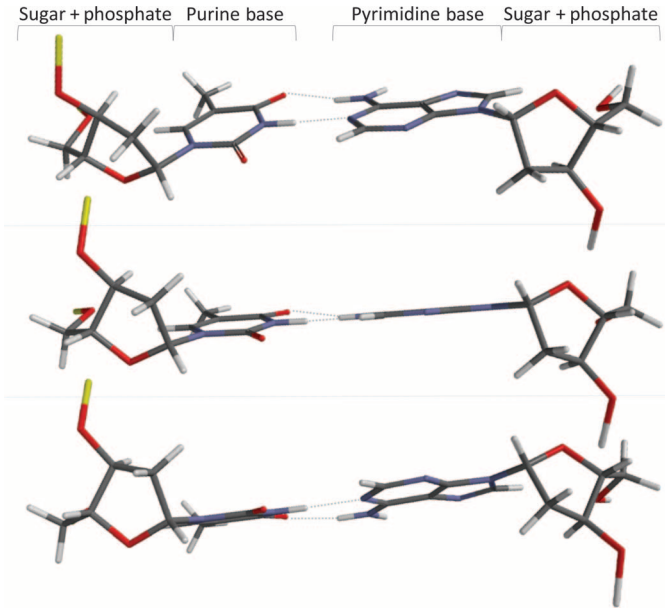

Fig. 2. Base propeller twist. A representative image of simulating different amounts of propeller twist of the A-T couple of bases in A-DNA is shown.

due to the positive propeller twist (*13*) of the bases with respect to the horizontal plane orthogonal to the DNA axis, as explicitly shown in Fig. 2. We also point out that in Table 1, the difference in length between the DNA diameter and the sum of the lengths of the base pairs and the backbone can be attributed to hydrogen bonds, which are between 2 and 3 Å, depending on the stretching state of the nucleotide in the helix position.

A-DNA HRTEM image simulation

To complete our analysis, in Fig. 3A, we report a numerical HRTEM simulation by the exit wave reconstruction method of a single dsDNA image formation, where the microscope parameters used (electron energy, beam current, spherical aberration coefficient, incidence semi-angle, and focus) are taken equal to those corresponding to the actual experimental conditions of our experiments. This simulation is realistic because our sample is background-free. Furthermore, in Fig. 3B, we report the front wave phase distortion (exit wave function) due to the phase change of the incidence plane wave under TEM conditions. This image helps in understanding the physical reason why a single DNA molecule gives enough phase change for a 1.5 Å resolution and a good image contrast. The phase shift modulation in a TEM is as follows:

$$\phi(x,y) = \frac{\pi t}{\lambda U_0}\Phi(x,y)$$

where $\phi(x, y)$ is the phase-contrast modulation of an object of thickness t (t = 21 Å for DNA) with atomic potential energy $\Phi(x, y)$, and the electron wavelength λ, in our case, is equal to 4.2 pm at U_0 accelerating energy of 80 keV. From the image simulation, we can see that after the TEM plane wave passes through 21 Å of DNA, the incidence wave function becomes distorted as $\phi(x, y)$ because of the atomic potential energy $\Phi(x, y)$ of the DNA molecule [$\phi(x, y)$, changes in the range of an appreciable fraction, 2π]. It is worth to say that this is under the hypothesis that spurious scattering from the substrate and from possible salt inclusions is absent. Both of these conditions are fulfilled by our preparation technique.

DISCUSSION

The determination of the structure of macromolecules is, without a doubt, in the realm of x-ray diffraction and other related techniques, such as small-angle x-ray scattering (SAXS) (*16*), grazing incidence SAXS, or nuclear magnetic resonance, for small molecules. The main limitation of x-ray diffraction is the necessity of having a crystal or a well-ordered fiber (*17*). Moreover, even under these conditions, the information obtained only refers to the particular crystal/fiber average configuration. All the details related to the modification at the level of a single molecule or to water environmental conditions cannot be seen in the crystal. For these and related reasons, the structural study of a single molecule is of fundamental importance because several biological processes and protein functions and their relations to pathology are strongly influenced by local molecular modification, such as epigenetic aspects (*18*, *19*) or point mutations (*20*).

Here, we demonstrate that a suspended single dsDNA molecule can be directly imaged by HRTEM at room temperature without additional molecular treatment and without negative or positive staining techniques by using heavy metal solutions. The TEM working conditions were chosen to minimize the damage due to knock-on and radiolysis (*1*) and to minimize any perturbation to the original biological structure. From the detection point of view, the present imaging was realized by accumulating a

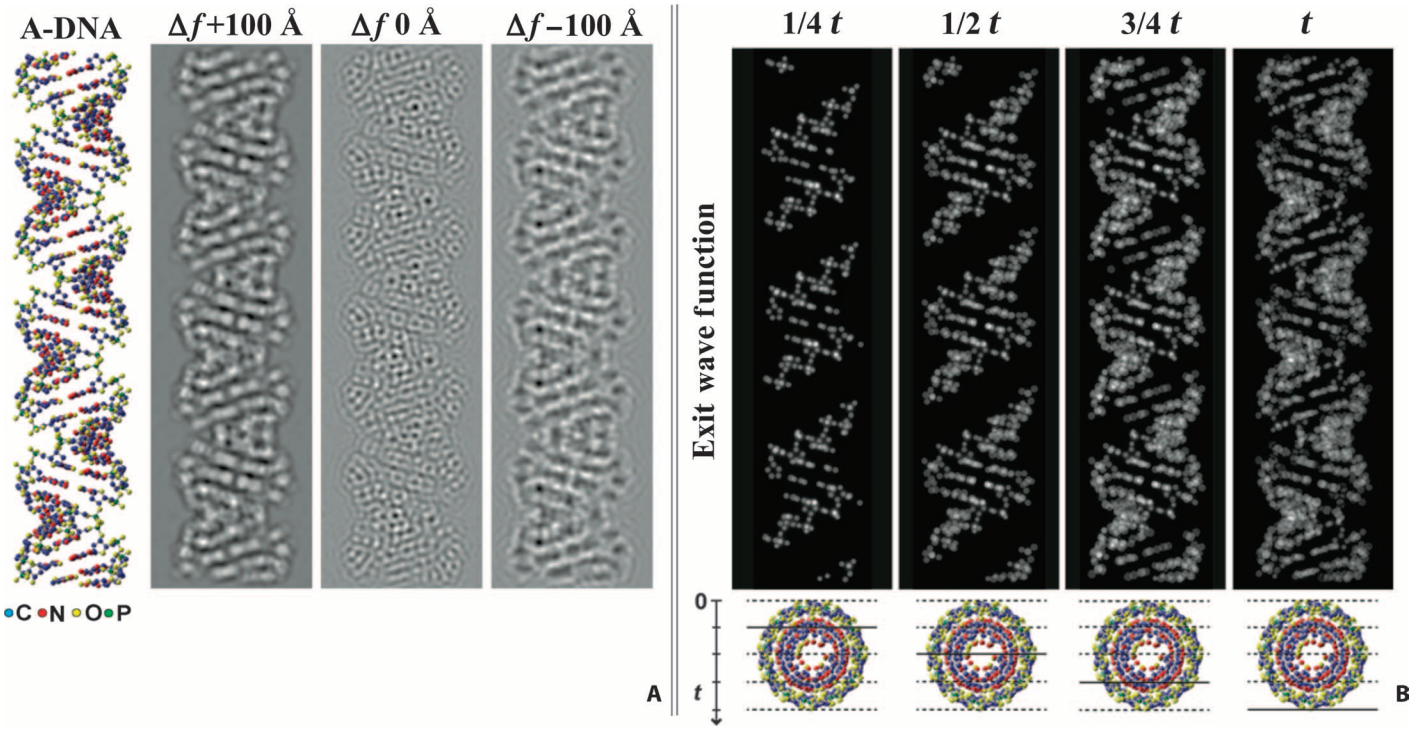

Fig. 3. A-DNA simulations. (**A**) Atomic model of A-DNA and corresponding HRTEM image simulations calculated using three defocus (Δ*f*) values. (**B**) The A-DNA filament was subdivided into four plane slices of ¼*t* = 6.0 Å parallel to the helix axis. The black arrow indicates the electron beam propagation direction perpendicular to the planes. The corresponding electron exit wave functions at ¼*t*, ½*t*, ¾*t*, and *t* show phase variations directly correlated to specimen potential and atom position. Amplitude changes are negligible due to weak phase object approximation. In both (A) and (B), the lattice fringes form angles of 18° with respect to the helix axis, and the periodicity of minor and major grooves is in accordance with the double-helix atomic model.

stack of two images. Moreover, we are aware of the development of detection cameras with sensitivity up to 100 times the one used in the present work. All these further improvements will represent additional handles to extend and improve both the final resolution and the contrast in imaging biological and radiation-sensitive materials. The present technique is fully compatible with cryo-TEM (*21*, *22*), and we expect that this can be combined to our approach to further improve the determination of protein structure. Some further consideration can be done about the possibility of performing DNA's TEM imaging by using an in situ sample holder with a dedicated cell for liquid samples, with the aim of providing complementary information about the DNA kept in a liquid environment. We point out that the imaging and metrological study reported here was possible because the forward scattering is negligible. We are not aware of other preparation methods with these characteristics. Even if the present method is compatible with samples in liquid solution (just adding an additional preparation step), the ultimate resolution of 1.5 Å that we achieved under our experimental conditions would be quite difficult to be reached because the electron beam should pass through both the two physical membranes that isolate the liquid cell from the vacuum of the TEM column and the whole thickness of the liquid constituting the solution containing DNA. Also, the intrinsic low contrast of the DNA is harder to be revealed if surrounded by a liquid solvent that has a similar scattering power but a much higher thickness. In the future, we suggest that this sample preparation would be fully compatible with free-electron laser investigation. Going back to the questions that triggered our research, the first three are positively answered by the present work, including the compatibility of the sample preparation with physiological conditions. Regarding the fourth question, we collected preliminary data, not shown in this work, where we confirm that our preparation protocol is fully compatible with the isolation and suspension of both genomic DNA from human samples and DNA after its interaction with the Rad51 repair protein. We are confident that in the near future, the present preparation technique will be extended to protein structural studies, where DNA can be used not only as a carrier of genetic information but also as the natural scaffold for direct imaging and manipulation of proteins (*23*–*26*). Finally, we want to clearly state that because of its intrinsic limited speed, the present approach is not intended as an alternative to the chemical sequencing of DNA but is relevant for structural studies. To resume our work on direct imaging of a single DNA molecule, we would like to conclude by paraphrasing a well-known sentence: "…eppur si vede" "nevertheless we see it" and measure it.

MATERIALS AND METHODS

DNA sample preparation

When a DNA fiber is stretched between μ-pillars, for its stability, we need to consider the adhesion force of DNA with pillars during the process of suspension. The partial helix dissociation of DNA due to the phosphate groups in the backbones gives the necessary adhesion force of DNA with silicon pillars. This force depends on the diameter of the fiber bundle and decreases with its radius. The minimum force is reached when a single dsDNA is suspended between pillars, because the electrostatic charge is at its minimum.

The preparation method (under patent evaluation) has been optimized to significantly increase the number of single well-stretched dsDNA detectable in each deposition; with the current efforts, we can routinely deposit bundles with diameters below 80 Å and more than 15 single dsDNA fibers per sample.

The nucleic acid object of investigation is the linear dsDNA (48,502 base pairs) isolated from bacteriophage λ (New England Biolabs) and stored in 1 mM EDTA and 10 mM tris-HCl (pH 8.0). This nucleic acid was chosen as a test sample because of its reproducibility, well-known sequence, and ease of handling. The total length of the dsDNA was a critical characteristic, theoretically allowing the stretching and suspension of only one molecule between μ-pillars with a 12-μm gap. Without further purification, the DNA solution was gently resuspended in the proper saline buffer [6.5 mM NaCl and 10 mM tris-HCl (pH from 6.5 to 9.3)] (*27*, *28*) to a final concentration of 50 ng/μl. The buffer used was a modification of the one previously reported in (*29*) and was filtered with a 0.2-μm filter (Millipore). The DNA solution was heated at 65°C for 10 min and then at 30°C until deposition. A 5-μl droplet of the freshly prepared diluted λ-DNA solution was deposited on a periodic circular lattice of silicon-based cylindrical μ-pillars with holes and left to evaporate at room temperature (23°C), 53% humidity, and standard pressure condition.

TEM operating conditions

HRTEM images are acquired on a Titan 60-300 electron microscope (FEI) equipped with a high-brightness electron gun (x-FEG), a Wien-type monochromator, a spherical aberration (C_S) corrector of the objective lens, and a Tridiem 865 Gatan image filter (GIF) coupled with an UltraScan 1000 2K × 2K charge-coupled device camera. The microscope is operated at 80-keV acceleration voltage. The beam is monochromated to an energy spread of about 120 meV (as measured by full width at half maximum of the zero-loss electron energy-loss spectroscopy peak). To compensate the residual C_S of fifth order and to improve the contrast of weak phase objects, the image corrector is operated with C_S of third order equal to −12 μm. To improve their contrast, the images are recorded on the GIF camera with the zero-loss filtering, thus filtering the inelastically scattered electrons, and the exposure time is from 0.3 to 1 s.

HRTEM image simulation conditions

The helical atomic structure of a dsDNA filament in its A-form (diameter of 22 Å) was obtained using the software UCSF Chimera version 1.10.1 by setting the arbitrary nucleotide sequence $d(GCGAAATTTGCG)_2$. A-DNA helix chains of 44 nucleotides were built to simulate the periodic arrangement of base pairs and to eliminate boundary effects at the apical ends of the chains. HRTEM images were calculated using MacTempas version 2.3.33, which is based on multislice approximation, whereby the DNA helical structure is subdivided into four phase-grating slices, each 6.0 Å thick, parallel to the helix axis. The helix structure was oriented with the slices perpendicular to the electron beam propagation. The specimen potential of $(n - 1)$-slice changes the amplitude and phase of traversing electron wave function, which is then transmitted onto the following (n)-slice where it is further modified through the whole structure. The "weak phase object" approximation of specimen potential is totally satisfied due to the low atomic number of DNA-forming atoms and the small specimen thickness (t) of few tens of angstrom. The HRTEM images were simulated considering an optical system with an acceleration voltage of 80 KeV, convergence angle of 0.55 mrad, defocus spread of 23 Å (due to the spread of the electron beam energy created by the variation of objective lens current, the spherical aberration of objective lens, the instabilities in high-voltage supply, and the intrinsic energy spread in the electron gun), and spherical aberration coefficient of −12 μm.

REFERENCES AND NOTES

1. R. F. Egerton, P. Li, M. Malac, Radiation damage in the TEM and SEM. *Micron* **35**, 399–409 (2004).
2. F. De Angelis, F. Gentile, F. Mecarini, G. Das, M. Moretti, P. Candeloro, M. L. Coluccio, G. Cojoc, A. Accardo, C. Liberale, R. P. Zaccaria, G. Perozziello, L. Tirinato, A. Toma, G. Cuda, R. Cingolani, E. Di Fabrizio, Breaking the diffusion limit with super-hydrophobic delivery of molecules to plasmonic nanofocusing SERS structures. *Nat. Photonics* **5**, 682–687 (2011).
3. E. Miele, A. Accardo, A. Falqui, M. Marini, A. Giugni, M. Leoncini, F. De Angelis, R. Krahne, E. Di Fabrizio, Writing and functionalisation of suspended DNA nanowires on superhydrophobic pillar arrays. *Small* **11**, 134–140 (2015).
4. F. Gentile, M. Moretti, T. Limongi, A. Falqui, G. Bertoni, A. Scarpellini, S. Santoriello, L. Maragliano, R. Proietti Zaccaria, E. di Fabrizio, Direct imaging of DNA fibers: The visage of double helix. *Nano Lett.* **12**, 6453–6458 (2012).
5. M. H. F. Wilkins, A. R. Stokes, H. R. Wilson, Molecular structure of nucleic acids: Molecular structure of deoxypentose nucleic acids. *Nature* **171**, 738–740 (1953).
6. E. Chargaff, Chemical specificity of nucleic acids and mechanism of their enzymatic degradation. *Experientia* **6**, 201–209 (1950).
7. L. Pauling, R. B. Corey, A proposed structure for the nucleic acids. *Proc. Natl. Acad. Sci. U.S.A.* **39**, 84–97 (1953).
8. J. D. Watson, F. H. C. Crick, Molecular structure of nucleic acids: A structure for deoxyribose nucleic acid. *Nature* **171**, 737–738 (1953).
9. R. E. Franklin, R. G. Gosling, Molecular configuration in sodium thymonucleate. *Nature* **171**, 740–741 (1953).
10. C. B. Carter, D. B Williams, *Transmission Electron Microscopy: A Textbook for Materials Science* (Springer-Verlag, New York, ed. 2, 2009), chap. 6, p. 108.
11. D. Voet, A. Rich, The crystal structures of purines, pyrimidines and their intermolecular complexes. *Prog. Nucleic Acid Res. Mol. Biol.* **10**, 183–265 (1970).
12. R. Taylor, O. Kennard, The molecular structures of nucleosides and nucleotides: Part 1. The influence of protonation on the geometries of nucleic acid constituents. *J. Mol. Struct.* **78**, 1–28 (1982).
13. E. Martin, W. Saenger, *Principles of Nucleic Acid Structure* (Springer-Verlag, Heidelberg, 1984).
14. R. E. Franklin, R. G. Gosling, The structure of sodium thymonucleate fibres. I. The influence of water content. *Acta Cryst.* **6**, 673–677 (1953).
15. W. Fuller, W.H.F. Wilkins, H.R. Wilson, L.D. Hamilton, The molecular configuration of deoxyribonucleic acid: IV. X-ray diffraction study of the *A* form. *J. Mol. Biol.* **12**, 60–76 (1965).
16. A. Accardo, L. Tirinato, D. Altamura, T. Sibillano, C. Giannini, C. Riekel, E. Di Fabrizio, Superhydrophobic surfaces allow probing of exosome self organization using X-ray scattering. *Nanoscale* **5**, 2295–2299 (2013).
17. M. H. Wilkins, R. G. Gosling, W. E. Seeds, Physical studies of nucleic acid: Nucleic acid: An extensible molecule? *Nature* **167**, 759–760 (1951).
18. L. Ellis, P. W. Atadja, R. W. Johnstone, Epigenetics in cancer: Targeting chromatin modifications. *Mol. Cancer Ther.* **8**, 1409–1420 (2009).
19. M. Hirst, M. A. Marra, Epigenetics and human disease. *Int. J. Biochem. Cell Biol.* **41**, 136–146 (2009).
20. G. Albrecht-Buehler, The spectra of point mutations in vertebrate genomes. *Bioessays* **31**, 98–106 (2009).
21. X. M. Li, P. Mooney, S. Zheng, C. R. Booth, M. B. Braunfeld, S. Gubbens, D. A. Agard, Y. F. Cheng, Electron counting and beam-induced motion correction enable near-atomic-resolution single-particle cryo-EM. *Nat. Methods* **10**, 584–590 (2013).
22. A. Bartesaghi, A. Merk, S. Banerjee, D. Matthies, X. Wu, J. L. Milne, S. Subramaniam, 2.2 Å resolution cryo-EM structure of β-galactosidase in complex with a cell-permeant inhibitor. *Science* **348**, 1147–1151 (2015).
23. A. A. Yu, T. Savas, S. Cabrini, E. di Fabrizio, H. I. Smith, F. Stellacci, High resolution printing of DNA feature on poly(methyl methacrylate) substrates using supramolecular nano-stamping. *J. Am. Chem. Soc.* **127**, 16774–16775 (2005).
24. M. Marini, L. Piantanida, R. Musetti, A. Bek, M. D. Dong, F. Besenbacher, M. Lazzarino, G. Firrao, A revertible, autonomous, self-assembled DNA-origami nanoactuator. *Nano Lett.* **11**, 5449–5454 (2011).
25. E. Torelli, M. Marini, S. Palmano, L. Piantanida, C. Polano, A. Scarpellini, M. Lazzarino, G. Firrao, A DNA origami nanorobot controlled by nucleic acid hybridization. *Small* **10**, 2918–2926 (2014).
26. M. R. Jones, N. C. Seeman, C. A. Mirkin, Programmable materials and the nature of the DNA bond. *Science* **347**, 1260901 (2015).
27. J. M. Gulland, D. O. Jordan, H. F. W. Taylor, Deoxypentose nucleic acids. Part II. Electrometric titration of the acidic and the basic groups of the deoxypentose nucleic acid of calf thymus. *J. Chem. Soc.* **25**, 1131–1141 (1947).
28. J. M. Creeth, J. M. Gulland, D. O. Jordan, Deoxypentose nucleic acids. Part III. Viscosity and streaming birefringence of solutions of the sodium salt of the deoxypentose nucleic acid of calf thymus. *J. Chem. Soc.* **25**, 1141–1145 (1947).
29. Y. Fujiyoshi, N. Uyeda, Direct imaging of a double-strand DNA molecule. *Ultramicroscopy* **7**, 189–192 (1981).
30. A. Vologodskii, *Biophysics of DNA* (Cambridge Univ. Press, Cambridge, 2015), chap. 1, pp. 6–7.

Funding: We acknowledge financial support from the King Abdullah University of Science and Technology start-up funding and from the Italian Ministry of Health under project nos. GR-2010-2320665 and GR-2010-2311677. **Author contributions:** E.D.F. conceived the whole project, participated in all phases (superhydrophobic conceiving, DNA solution, TEM imaging, and data analysis), and wrote the manuscript; M. Marini conceived the project; participated in DNA preparation, TEM imaging, and data analysis; performed experiments; and contributed to manuscript writing; A.F. did TEM measurements and TEM simulation and contributed to manuscript writing; M. Moretti and T.L. participated in setting the DNA solution and its suspension; M.A. realized the superhydrophobic devices; A. Genovese did TEM image simulation; S.L. performed TEM measurements and imaging optimization; L.T. participated in DNA suspension optimization and setting of the DNA solution; G.D. participated in preparation optimization of the sample and its purification through Raman scattering; B.T. and A. Giugni participated in preparation optimization of the sample and its drying on superhydrophobic substrate; and F.G. and P.C. participated in the realization and optimization of the superhydrophobic devices. All the authors discussed and commented on the manuscript. **Competing interests:** The authors declare that they have no competing interests. **Data and materials availability:** The data for the reported analyses are available upon request from the corresponding author.

Submitted 6 June 2015
Accepted 13 July 2015
Published 28 August 2015
10.1126/sciadv.1500734

Citation: M. Marini, A. Falqui, M. Moretti, T. Limongi, M. Allione, A. Genovese, S. Lopatin, L. Tirinato, G. Das, B. Torre, A. Giugni, F. Gentile, P. Candeloro, E. Di Fabrizio, The structure of DNA by direct imaging. *Sci. Adv.* **1**, e1500734 (2015).